NANO LETTERS

2006
Vol. 6, No. 8
1757−1760

Transient Grating Measurements of Excitonic Dynamics in Single-Walled Carbon Nanotubes: The Dark Excitonic Bottleneck

H. Ye. Seferyan,[†] M. B. Nasr,[†] V. Senekerimyan,[†] R. Zadoyan,[†] P. Collins,[‡] and V. A. Apkarian*,[†]

Department of Chemistry, University of California, Irvine, California 92697, and Department of Physics and Astronomy, University of California, Irvine, California 92697

Received July 17, 2006

ABSTRACT

Transient grating measurements affirm the excitonic model for single-walled carbon nanotubes (SWNT) by identifying the dark exciton (D) as the population relaxation bottleneck in semiconducting-SWNT (S-SWNT). The data allow the reconstruction of the kinetics of excitonic cascade and cooling, from band continuum to vibrational cooling in the ground electronic state. In S-SWNT, the intraband relaxation occurs in 40 fs, localization into the 2_g exciton occurs in 50 fs, followed by the excitonic cascade: $2_g \rightarrow 1_u \rightarrow D \rightarrow 1_g$ with time constants of 175 fs, 3 ps, 300 ps, respectively. Fluorescence from the 1_u state is quenched by efficient population transfer to ^1D dark exciton. In metallic tubes, cooling is completed on the time scale of 1 ps.

Because of their small diameter (≈1 nm) and extended dimension along the tube axis, single-walled carbon nanotubes (SWNTs) are characterized as quasi-one-dimensional charge carriers,[1] with very low resistance.[2] A significant body of spectroscopic studies has been undertaken to derive a fundamental description of the electronic structure and dynamics of SWNT, mindful of potential applications as ultracompact and narrow-band emitters and detectors. In addition to fluorescence[3−5] and electroluminescence,[6] time-resolved photoemission[7−9] and pump−probe measurements[10−17] have been carried out. Although initially the framework of the band structure derived from tight-binding treatments (Huckle theory) was adopted, both theoretical refinement and experimental evidence increasingly point to the excitonic picture as the more appropriate description. Rather than free charge carriers, electron−hole correlation should be enhanced by confinement to low dimensionality.[18] Indeed, two-photon spectroscopy convincingly demonstrates that in semiconducting tubes (S-SWNT) localized excitonic states occur within the fundamental band gap.[19] The measurements locate two gap states: the two-photon accessible 2_g state located above the fluorescing 1_u state, both possessing e−h binding energies that are a significant fraction of the band gap (see Figure 1). Rather than simple Huckle theory, electron correlation through configuration interaction is essential for a realistic description of the states that arise from the sp^2 carbon orbitals.[20] A variety of refined treatments has appeared,[21−24] including the semiempirical PPP−Hamil-

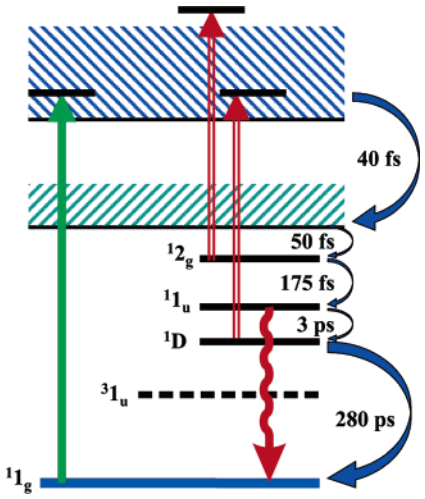

Figure 1. Energy level diagram and relaxation pathways for S-SWNT. The single-straight green arrow depicts the pump, and the double-straight red arrow, the probe. The oscillator strengths of the transitions are concentrated on selected states within the respective excitonic manifolds (black horizontal lines).

* To whom correspondence should be addressed. E-mail: aapkaria@uci.edu.
[†] Department of Chemistry.
[‡] Department of Physics and Astronomy.

10.1021/nl061646d CCC: $33.50
Published on Web 07/26/2006

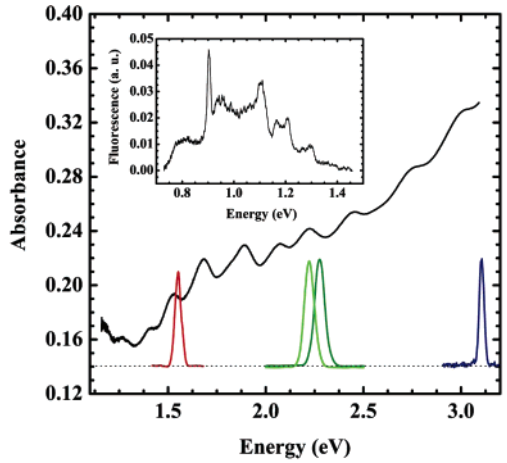

Figure 2. Linear optical absorption of SWNTs in water. Spectra of the excitation (2.23 eV, 2.28 eV) and probe (1.53 eV, 3.06 eV) pulses used in the measurements. The inset shows the fluorescence spectrum of our sample, obtained by excitation at 532 nm, with 7 ns pulses. The spike at 0.9 eV is an artifact (scattered YAG light from the suspension).

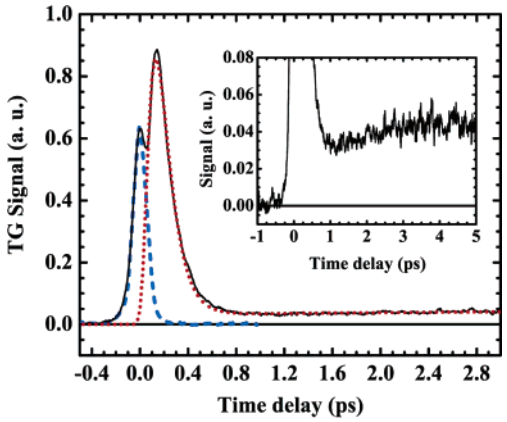

Figure 3. TG signal, excited at 2.23 eV and probed at 1.53 eV (solid line), together with the fit (red dotted line) according to the discussed model. Identical results are obtained when excited at 2.28 eV. Blue dashed line shows three-beam cross correlation in a 0.2 mm sapphire substrate. The formation of a valley between the nonresonant response peak and the sharp peak that follows, necessarily implies that the observed population rise is subject to an induction time—that the observed state (assigned $^1 2_g$, see text) is sequentially populated. The fit assumes an intermediate state with rise and fall times of 40 and 50 fs, respectively; and a decay time of 175 fs for the population in $^1 2_g$. The inset illustrates the observed 3 ps rise of population in the ^{1}D-state.

tonian[25] that has been extensively calibrated in treatments of conjugated organic polymers to extract energetics and transition moments of the excitonic states.[26,27] A dark excitonic state is predicted below the radiative state due to the e−e induced splitting of the degeneracy that exists in the uncoupled limit.[28] Moreover, in accord with the general rule, the triplet exciton $^3 1_u$ is to be expected as the lowest excited π^*-state, as in π-conjugated systems.[29] The energetics and roles of these states in excited state dynamics are poorly understood. Our transient grating (TG) measurements clearly demonstrate the presence of an electronic bottleneck below the optically active exciton. Based on the strength of its coupling, the state is most consistent with the singlet dark exciton rather than the triplet state. Besides affirmation of the excitonic model, our analysis allows reconciliation of seemingly contradictory observations made in time-resolved spectroscopy.

We investigate SWNT suspensions in water. The SWNT, obtained from NanoSelect Inc., are prepared by the high-pressure CO (HiPCO) method and processed in a manner similar to that described in ref 3: they are unbundled by vigorous sonication, separated by centrifugation and wrapped in sodium dodecyl sulfate (SDS) micelles to solubilize in water and prevent reaggregation. Inspection of the sample under an atomic force microscope (AFM) shows a distribution of lengths that range between 50 and 500 nm, with a mean centered near 200 nm, and an estimated typical diameter of 0.8 nm. The absorption spectrum of the aqueous solution is shown in Figure 2. The laser induced fluorescence spectrum obtained by excitation at 532 nm, is shown in the inset to Figure 2. The resolved structure of peaks is a signature of isolated SWNT, characteristic of the distribution of chirality and tube radii obtained with the preparation that has become a standard in spectroscopic applications.[3]

We carry out four-wave mixing measurements on a windowless film of the aqueous SWNT solution. The solution is circulated with a peristaltic pump to sustain a gravity-driven wire-guided liquid jet, similar to that described in ref 30. We use a 200 μm Tungsten wire-guide, and estimate the thickness of the membrane in the excitation volume to be 50 μm. The samples are diluted enough to ensure that the measured signals are independent of concentration. The laser system used is a regeneratively amplified Ti:Sapphire laser (1.53 eV photons, at 1 kHz, 0.5 mW, 70 fs), which pumps a traveling wave optical parametric amplifier to generate visible pulses (2.0−2.43 eV photons, compressed to 45 fs). The boxcar geometry is employed, in which three noncollinear beams are brought to focus through a single achromatic lens. The signal beam is detected after spatial filtering. To minimize background due to diffuse light scattering from the suspension, one of the pump beams is synchronously chopped and the signal is boxcar integrated in the active baseline subtraction mode to yield a signal-to-noise ratio of 5000:1. A variety of pulse sequences were used in the four-wave mixing measurements to establish that electronic dephasing is faster than our experimental time resolution of 70 fs. The most instructive data are obtained from TG measurements, in which the interference between a coincident pair of green pulses (2.23 or 2.28 eV) is used to write a polarization grating, and a time delayed probe pulse at 1.53 or 3.06 eV is used to read it. The spectra of pulses used are shown in Figure 2. It can be seen that 2.23 and 2.28 eV photons overlap with a peak and valley in the absorption band. The results obtained with gratings prepared with either color are indistinguishable. The most informative data set is obtained with the IR probed TG, which is shown on picosecond and nanosecond time scales in Figures 3 and 4.

The homodyne TG signal measures the modulus squared of third-order polarization $|P^{(3)}(t)|^2$.[31] Three distinct components can be seen at early time, in Figure 3: an initial

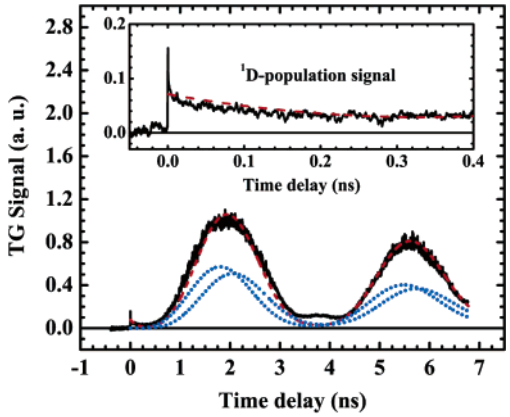

Figure 4. Acoustic grating signal and the long-lived ^{1}D-population signal (expanded in inset). The dashed red line is the theoretical fit, and the dotted blue lines are the decomposition into slow (S-SWNT) and fast (M-SWNT) components.

response limited component that is dominated by the electronic response of the solvent, followed by a buildup and decay of population in an intermediate state that is completed in ≈400 fs, followed by a rise on the time scale of 3 ps that is highlighted by the expansion in the inset. The latter component decays on the time scale of 10^2 ps and leads to the acoustic grating that oscillates with a period of 4 ns, as seen in Figure 4. The data are sufficient for a complete reconstruction of the population cascade, which at 2.23 eV excitation starts from the second excitonic manifold (E_{22} in the tight-binding model). We provide an explicit analysis, starting with the acoustic component.

The acoustic signal serves as a calorimetric probe. Its rise time and shape are determined by the heating rate of the solvent—the rate at which the internal excitation energy of SWNT is converted to translational energy of water molecules. The scattered beam on nanosecond time scales is strictly due to the real part of the third-order polarization, due to the index grating that tracks the density profile of the liquid. The density wave is launched by the inhomogeneous heating profile set up by the interference pattern with fringe spacing $d = \lambda/[2 \sin(\theta/2)]$, in which θ is the coincidence angle between the pump beams and λ is the wavelength. The acoustic breathing of the density wave controls the oscillations of the TG signal, with a period $\tau = d/2v$, where v is the speed of sound. The conductivity equations can be solved explicitly to simulate the signal.[32] Because the conductivity constants of water are well-known, the only fitting parameter in the analysis of the signal is the heating rate of the solvent. To fit the broadened profile, it is essential to assume two distinct cooling channels of comparable strengths: an instantaneous channel with a time constant of ≈1 ps, and a slower channel with a time constant of 280 ps. The decomposition of the signal into these two components is shown in Figure 4. The slow component leads to the discernible peak shift in the acoustic signal. The rate of the slow heating channel matches the exponential decay of the population grating that precedes the acoustic wave (Figure 4, inset), establishing that the observed population decay is the rate-limiting step of cooling. The fast and slow contributions can be associated respectively with the cooling rates of metallic (M-SWNT) and semiconducting nanotubes, which are present with a statistical probability in the HiPCO preparation. Because the optical excitation to the excitonic continuum is indiscriminate, both M-SWNT and S-SWNT are excited and must contribute to the acoustic signal. The cooling of M-SWNT has been established through time-resolved photoemission[7] and photoelectron spectroscopy[33] to be completed in several picoseconds. We may therefore conclude that the slow channel represents the cooling of S-SWNT and that the bottleneck is electronic in origin. The population in the bottleneck state is directly observed to rise in 3 ps and to decay in 280 ps. The rise time corresponds to the nonradiative decay time of the fluorescing 1_u state, previously measured through photon up-conversion and Kerr gating.[89] Evidently, the 1_u state is quenched by population transfer to the bottleneck state. In principle, both the singlet D-exciton and the triplet exciton can act as bottleneck. However, the fast transfer time of 3 ps cannot be reconciled with the week spin−orbit coupling in the light carbon atom network, where typical intersystem crossing rates are 10^6−10^7 s^{-1}.[34] Therefore, with some confidence, we may assign the bottleneck to the theoretically predicted singlet dark exciton (^{1}D).[28] As a corollary, we may conclude that the triplet state is entirely circumvented in the process of relaxation down to the ground electronic state.

The kinetics of the population cascade can be retraced to the time origin by considering the signal in Figure 3. The peak at $t = 0$ is dominated by the instantaneous electronic response of the solvent—its profile is identical to what is seen in neat water. This electronic grating serves to calibrate the experimental time resolution as 70 fs. The subsequent population-grating signal can be fitted after convolution with the experimental response function:

$$I_{TG}(t) = \left(\int_{-\infty}^{\infty} dt'\, e^{-((t-t')/\Delta)^2} \sum_i \sigma_i(\lambda)\, N_i(t')\right)^2 \qquad \text{with} \quad \Delta = 70 \text{ fs} \quad (1)$$

in which σ_i are transition cross sections of participating states i at the probe wavelength λ, with time dependent populations N_i. The entire signal is reproduced by assuming contributions from only two states with a 1:4 ratio of cross sections. The weak component, with 3 ps rise and 280 ps fall, was already assigned above to ^{1}D (see Figure 1). The stronger component gives rise to the peak observed at a delay of 150 fs, which decays with a time constant of 175 fs. To form a peak distinct from the instantaneous response, it is essential that there be an induction time in the buildup of the population in the observed state. An induction period, in turn, implies that the state is populated sequentially. The minimal model required to reproduce the signal must assume that the population promoted to the band continuum relaxes in 40 fs to an intermediate state, which in 50 fs populates the observed state. That the initially pumped state decays in time shorter than our experimental resolution, we have verified by delaying the two pump pulses relative to each other. The 40 fs decay rate of the initial state, as extracted from the best fit to the data, is in excellent agreement with a prior

observation and assignment to intraband relaxation.[17] Accordingly, we may conclude that the observed state is below the band edge. Moreover, the 175 fs decay of this state corresponds to the previously measured rise time of population in the 1_u state, suggesting that it is above the 1_u state and feeds directly into it. Rather uniquely, the observed state may be identified as the 2_g. This assignment completes the map of the population cascade shown in Figure 1. The population promoted to the band continuum at 2.3 eV relaxes to the band edge in 40 fs, localization into the excitonic 2_g state occurs in 50 fs, followed by the excitonic cascade: $2_g \rightarrow 1_u \rightarrow D \rightarrow 1_g$ with time constants of 175 fs, 3 ps, 280 ps, respectively.

The derived kinetic scheme allows rationalization of much of the previous time-resolved spectroscopic observations. In particular, long-lived transients, with decay times ranging between 100 and 500 ps have been reported in a variety of pump−probe experiments.[8,14,15] In the earlier reports, which assumed the tight-binding framework in their discussions, the long-lived component has been associated with population at the band edge of the fundamental gap.[14] An argument used for this assignment is that the transient is seen when the excitation is resonant with peaks near the absorption threshold and absent when valleys are excited, to suggest that the state can only be prepared when the band edge is accessed. This is contradicted by the fact that in the present, the excitation at 2.3 eV is far from the fundamental gap. Moreover, whether we excite a peak or a valley in the absorption profile, at 2.23 and 2.28 eV, the identical signals are observed as required by the model extracted from the kinetic analysis. Rather than the pump wavelength, the visibility of the ^{1}D state can be understood in terms of the probe resonances, recognizing that strong optically coupled states occur within a given excitonic manifold.[28,29] Indeed, this is clearly demonstrated in pump−probe measurements where the probe wavelength is scanned and a modulated spectrum is obtained for the long-lived component.[15] We ascribe those spectra to absorptions starting from the ^{1}D-state, rather than band-edge excitations of different SWNT. The more recent experiments and theoretical analysis by Mazumdar[29] are in good accord with our interpretation. Finally, we should point out that the interpretation of transient absorption is complicated by the chiral distribution of nanotubes in a given preparation, and the fact that several manifolds of transitions from a given SWNT overlap spectrally. Of the several colors studied, we have selected the data set that allows the most direct interpretation, by virtue of the fact that optical transitions with only two initial states, $^1 1_g$ and ^{1}D states, dominate the absorption at the probe wavelength.[29] At probe wavelengths where the ground-state absorption dominates, instantaneous recovery of the photobleach is observed,[14,15] which we attribute to recovery in M-SWNT—transient absorption does not distinguish between metallic and semiconducting nanotubes. Key to the resolution of this seeming contradiction is the calorimetric information content in the acoustic grating data. We clearly observe two populations with distinct cooling times of 1 and 300 ps (recovery of the thermalized ground state), which we assign to the M- and S-SWNT, respectively. Finally, although the triplet exciton is expected to be the lowest in energy, the optically excited population seems to completely circumvent it.

Acknowledgment. We thank Dr. Kazuki Yoshioka for help during the measurements.

References

(1) Dresselhaus, M. S.; Dresselhaus, G.; Avouris, Ph. *Carbon Nanotubes: Synthesis, Structures and Applications*; Springer-Verlag: Berlin, 2001.
(2) Li, S.; Yu, Z.; Rutherglen, C.; Burke, P. J. *Nano Lett.* **2004**, *4*, 2003.
(3) O'Connel, M. J.; et al. *Science* **2002**, *297*, 593.
(4) Hartschuh, A.; et al. *Science* **2003**, *301*, 1354.
(5) Htoon, H.; et al. *Phys. Rev. Lett.* **2005**, *94*, 127403.
(6) Misewich, J. A.; et al. *Science* **2003**, *300*, 783.
(7) Hertel, T.; Moos, G. *Phys. Rev. Lett.* **2000**, *84*, 5002.
(8) Ma, Y.-Z.; et al. *J. Chem. Phys.* **2004**, *120*, 3368.
(9) Wang, F.; et al. *Phys. Rev. Lett.* **2004**, *92*, 177401.
(10) Chen, Y. C.; et al. *Appl. Phys. Lett.* **2002**, *81*, 975.
(11) Han, H.; et al. *Appl. Phys. Lett.* **2003**, *82*, 1458.
(12) Lauret, J. S.; et al. *Phys. Rev. Lett.* **2003**, *90*, 057404.
(13) Korovyanko, O. J.; et al. *Phys. Rev. Lett.* **2004**, *92*, 017403.
(14) Ostojic, G. N.; et al. *Phys. Rev. Lett.* **2004**, *92*, 117402.
(15) Huang, L.; Pedrosa, H. N.; Krauss, T. D. *Phys. Rev. Lett.* **2004**, *93*, 017403.
(16) Ma, Y.-Z.; et al. *Phys. Rev. Lett.* **2005**, *94*, 157402.
(17) Manzoni, C.; et al. *Phys. Rev. Lett.* **2005**, *94*, 207401.
(18) Ogawa, T., Kanemitsu, Y., Eds. *Optical properties of low-dimensional materials*; World Scientific Publishing: Singapore, 1995.
(19) Wang, F.; et al. *Science* **2005**, *308*, 838.
(20) Ando, T. *J. Phys. Soc. Jpn.* **1997**, *66*, 1066.
(21) Chandross, M.; et al. *Phys. Rev. B* **1999**, *59*, 4822.
(22) McWilliams, P. C. M.; Hayden, G. W.; Soos, Z. G. *Phys. Rev. B* **1991**, *43*, 9777. Race, A.; Barford, W.; Bursill, R. J. *Phys. Rev. B* **2001**, *64*, 035208.
(23) Rice, M. J.; Gartstein, Yu. N. *Phys. Rev. Lett.* **1994**, *73*, 2504.
(24) Perebeinos, V.; Tersoff, J.; Avouris, P. *Phys. Rev. Lett.* **2005**, *94*, 027402.
(25) Pariser, R.; Parr, R. G. *J. Chem. Phys.* **1953**, *21*, 466. Pople, J. A. *Trans. Faraday. Soc.* **1953**, *49*, 1375.
(26) Leng, J. M.; et al. *Phys. Rev. Lett.* **1994**, *72*, 156. Frolov, S. V.; et al. *Phys. Rev. Lett.* **2000**, *48*, 2196.
(27) Weiser, G. *Phys. Rev. B* **1982**, *45*, 14076. Guo, D. *Phys. Rev. B* **1993**, *48*, 1433. Liess, M.; et al. *Phys. Rev. B* **1997**, *56*, 15712.
(28) Zhao, H.; Mazumdar, S. *Phys. Rev. Lett.* **2004**, *93*, 157402.
(29) Zhao, H.; et al. *Phys. Rev. B* **2006**, *73*, 075403.
(30) Tauber, M. J.; et al. *Rev. Sci. Instrum.* **2003**, *74*, 4958.
(31) Xu, Q.; Ma, Y.; Fleming, G. R. *Chem. Phys. Lett.* **2001**, *338*, 254.
(32) Kimura, Y.; et al. *J. Chem. Phys.* **2005**, *123*, 054512.
(33) Hertel, T.; Fasel, R.; Moos, G. *Appl. Phys. A* **2002**, *75*, 449.
(34) McGlynn, S. P.; Azumi, T.; Kinoshita, M. *Molecular Spectroscopy of the Triplet State*; Prentice-Hall: Englewood Cliffs, NJ, 1969.

NL061646D